International Journal of Science and Research (IJSR)
ISSN: 2319-7064
SJIF (2020): 7.803

Chemical Synthesis of Nickel Oxide Thin Film and Study of Structural and Electrochemical Properties

Ganesh Vasant Dilwale

Department of Physics, RNC Arts, JDB Commerce and NSC Science College Nashik Road Maharashtra – 422101, India
Email: *dilwaleganesh10[at]gmail.com*

Abstract: ***Nickel oxide (NiO) is one of the most positive anode materials for electrochemical supercapacitor. The material is directly deposited on the stainless - steel substrate during the hydrothermal reaction process. Depositions were carried out in temperature range of 80^{o}C to 100^{o}C for 20 hours to 24 hours. Optimized thin films were further characterized for Phase, morphologies, elemental analysis, quantitative compositional information and functional groups were characterized by X- ray diffraction (XRD), scanning electron microscopy (SEM). The specific capacitance of 470 Fg^{-1} at scan rate 10 mV/sec was achieved using cyclic voltammetry and 470 Fg^{-1} at 1 Ag^{-1} current density from galvanostatic charge and discharge curves.***

1. Introduction

At present world facing major problems of over population and global economy due to this demand for energy consumption has been tremendously increased. Supercapacitor devices are emerging as one of the promising energy devices for the future energy technology [1]. Metal oxides are very good sensing materials. In the recent years metal oxide nanostructures have been extensively studied in order to optimize them for several applications, including gas sensing and energy storage devices. There are three important factors on which performance of supercapacitor mainly depends on namely electrochemical properties of the electrode material, electrolyte and voltage range [2]. In this paper, storage mechanism of supercapacitors with their types, characteristics of the electrode material, different synthesis methods of nickel oxide electrode material and different electrolyte materials have been reported [3]. The hydrothermal chemical method is a simple method which is employed for the deposition of materials [4]. Semiconducting n - type metal oxides have been reported as energy storage material very deeper than their p - type counterparts [5]. Recently, also p - type metal oxides are being studied, and among them nickel oxide (NiO) [6]. As an important p - type semiconductor with wide band gap energy in the range of 3.6–4.0 eV [7]. Till date, various NiO nanostructures have been grown, including nanoparticles [8], nanorods [9], nanotubes [10], and nanosheets [11].

2. Experimental Section

2.1 Materials preparation

The NiO nanowires have synthesised hydrothermal method followed by an annealing at 400^0C All the chemicals used in our experiments were of analytical reagent grade and were directly used without further purification. In the experimental work, 0.486 g of $NiCl_2.6H_2O$was dissolved into a mixture of 32 mL ethylene glycol and 18 mL deionized water in a beaker under continuous magnetic stirring at room temperature. Then 0.1206 g of $Na_2C_2O_4$ was added into the beaker. An hour of continuous magnetic stirring was carried out to ensure that Ni^{2+} ions were dispersed homogeneously in the solution. The clear solution was transferred into a Teflon - lined stainless - steel autoclave of 120 mL capacity. The autoclave was sealed and heated at 180^0C for 18 h. After the heating treatment, the autoclave was left for cooling to room temperature naturally. The product was collected by centrifugation, washed with several times with deionized water and then dried in air. As a result, a blue–green product was obtained. The polycrystalline NiO nanowires were obtained by the calcination of this blue - green precursor, consisting in nickel oxalate hydrate ($NiC_2O_4.2H_2O$) short nanowires, at 400^0C. The as - prepared material and the calcinated nanowires were characterized and analyzed by using X - ray diffraction (XRD) and scanning electron microscopy (SEM).

3. Material Characterizations

3.1 X - ray diffraction

A confirmation about the composition of the nanowires before and after the calcination is given by the X - ray diffraction spectra shown in Figure 1. In Figure 1, relative to nanowires after the calcination process, shows instead a well crystallized cubic NiO phase (JCPDS 47 - 1049). The three intense diffraction peaks at 37.1, 43.2, and 62.7 degree can be indexed to its cubic unit cell, with a lattice parameter of $4.231A^0$. The absence of peaks for any impurity phase in XRD spectra of Figure 1 confirms that the nanostructures are pure crystals and that the $NiC_2O_4.2H_2O$ precursor was completely converted to NiO during calcination.

The peaks are very sharp which indicate good crystallinity of material. The crystallite size is obtained as follows,

$$\beta_T = \frac{k\lambda}{D\cos\theta} + 4\epsilon\tan\theta \quad (1)$$

where, λ is wavelength of Cu $(k_\alpha = 0.154060\ nm)$ radiation, ϵ is strain, shape factor$k = 0.9$ and θ is angle of diffraction. Crystallite size (D). From the XRD data of NiO the average crystallite size is calculate as **56 *nm*** , the strain ϵ= 0.00124 and dislocation density **δ= 1.876869 X 10^{-3} (*nm*)$^{-2}$**

4. Electrochemical Performance

4.1 Cyclic Voltammetry (CV)

Figure 5 shows CV curves of Nickel oxide nanoparticles at the scan rate10 mVs $^{-1}$ in 1 M KOH electrolyte. It is clear from redox reaction peaks that the material exhibits pseudocapacitive behaviour. The redox peaks arise within the potential range - 0.4 to - 1.0 V (vs Ag/AgCl), which is due to reversible electrochemical reactions. The specific capacitance of nickel oxide nanoparticles is calculated from following equations [12].

$$C = \frac{I \times \Delta t}{M \times \Delta E} \quad (2)$$

$$\text{Specific energy} = \frac{I \times V \times \Delta t}{M} \quad (3)$$

$$\text{Specific power} = \frac{I \times V}{M} \quad (4)$$

Where C is the specific capacitance (Fg $^{-1}$), I is the current density (A), Δ *t* is the discharging time, M is the active mass of electrode (g) and ΔE is the voltage change after full discharge (V), *V* is voltage window, Specific energy (whkg $^{-1}$) and Specific power (Wkg $^{-1}$). From equation (2) the specific capacitance values calculated for Nickel oxide nanoparticleswere 530, 448, 382, 365, 351 and 340 Fg $^{-1}$ at the current densities 1.0, 1.25, 1.50, 1.75, 2.0 and 2.25 Ag $^{-1}$, respectively. The specific capacitance as a function of current densities is shown in figure 2 (c). The specific capacitance decreased exponentially with increasing current density. The diffusion of ions towards the surface of the electrode lowers with increased current density which affects the value of specific capacitance. At low current density the material attains maximum specific capacitance due to its fast charge transfer at the interface of electrolyte and electrode surface. The energy densities in Whkg $^{-1}$ and power densities in Wkg $^{-1}$ are calculated from equations (3) and (4). The energy density verses power density 'ragone plot' is shown in figure 3). At different current densities from 1.0 to 2.25 Ag $^{-1}$ the power density increased from 548.5 to 1236.71Wkg $^{-1}$ and energy density decreased from 87.8 to 51.18 Whkg $^{-1}$. We have achieved maximum specific capacitance of 470 Fg $^{-1}$ at current density of 1 Ag $^{-1}$ from galvanostatic charging - discharging curve.

5. Conclusions

We have grown Ni - O nanowires via a simple and cheap process consisting in hydrothermal growth followed by high temperature calcination. The specific capacitance of 470 Fg $^{-1}$ at scan rate 10 mV/sec was achieved using cyclic voltammetry and 470 Fg $^{-1}$ at 1 Ag $^{-1}$ current density from galvanostatic charge and discharge curves.

References

[1] R. S. Kate, S. A. Khalate, R. J. Deokate, Journal of Alloys and Compounds 734 (2018).
[2] F. Luan, G. Wang, Y. Ling, X. Lu, H. Wang, Y. Tong, X. - X. Liu, Y. Li, Nanoscale 5 (2013).
[3] Y. Xie, C. Huang, L. Zhou, Y. Liu, H. Huang, Composites Science and Technology 69 (2009).
[4] K. Nguyen, N. D. Hoa, C. M. Hung, D. T. Thanh Le, N. van Duy, N. van Hieu, RSC Advances 8 (2018).
[5] T. F. Yi, T. T. Wei, J. Mei, W. Zhang, Y. Zhu, Y. G. Liu, S. Luo, H. Liu, Y. Lu, Z. Guo, Advanced Sustainable Systems 4 (2020).
[6] M. D. Irwin, D. B. Buchholz, A. W. Hains, R. P. H. Chang, T. J. Marks, Proceedings of the National Academy of Sciences 105 (2008).
[7] A. Heinzig, T. Mikolajick, J. Trommer, D. Grimm, W. M. Weber, Nano Letters 13 (2013).
[8] E. R. Beach, K. Shqau, S. E. Brown, S. J. Rozeveld, P. A. Morris, Materials Chemistry and Physics 115 (2009).
[9] N. Srivastava, P. C. Srivastava, Physica E: Low - Dimensional Systems and Nanostructures 42 (2010).
[10] S. A. Needham, G. X. Wang, H. K. Liu, Journal of Power Sources 159 (2006).
[11] Z. - H. Liang, Y. - J. Zhu, X. - L. Hu, The Journal of Physical Chemistry B 108 (2004).
[12] V. Srinivasan, J. W. Weidner, Journal of The Electrochemical Society 147 (2000).

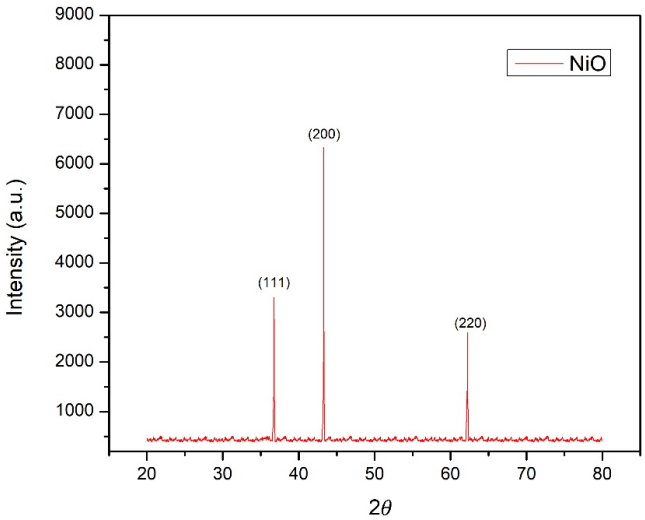

Figure 1: XRD of Nickel oxide

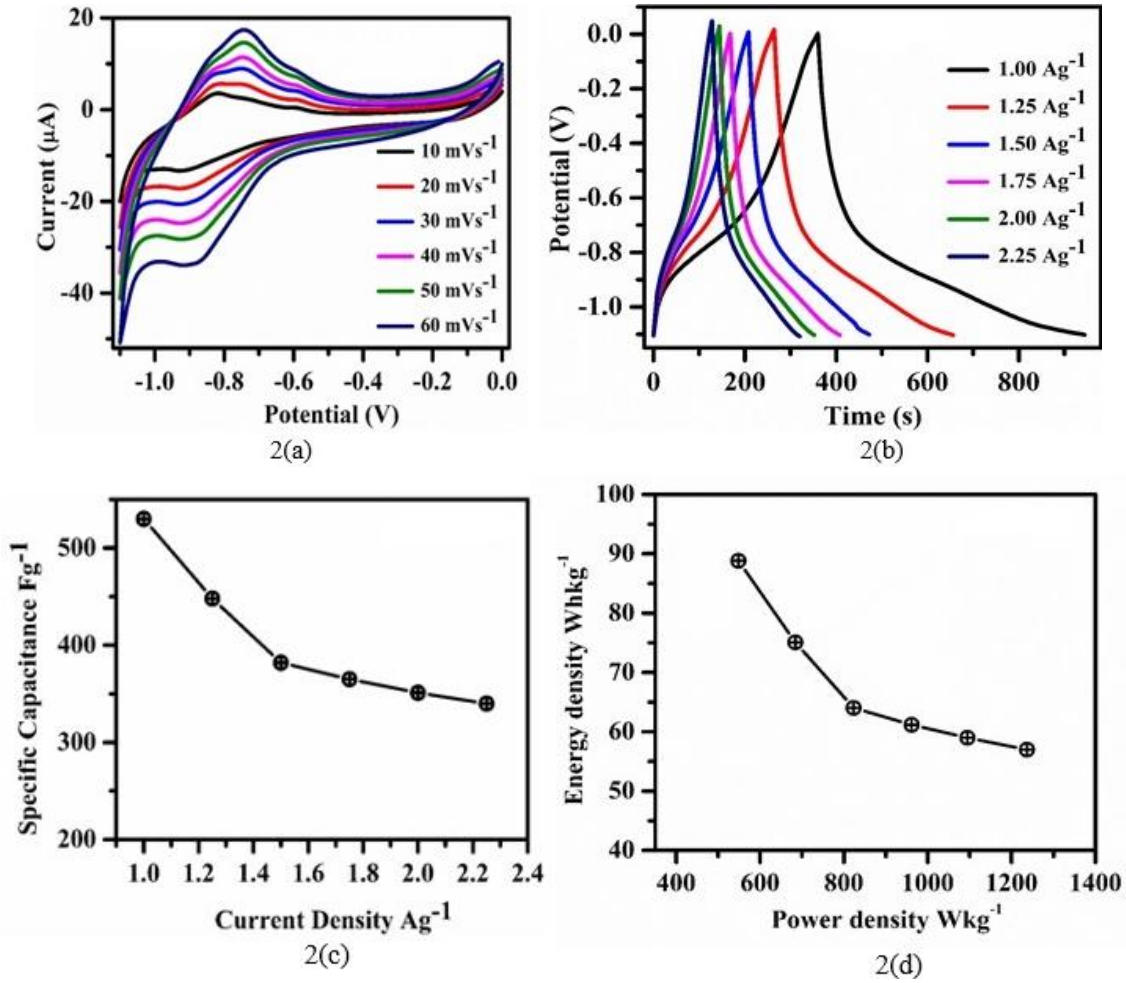

Figure 2: CV of Nickel oxide

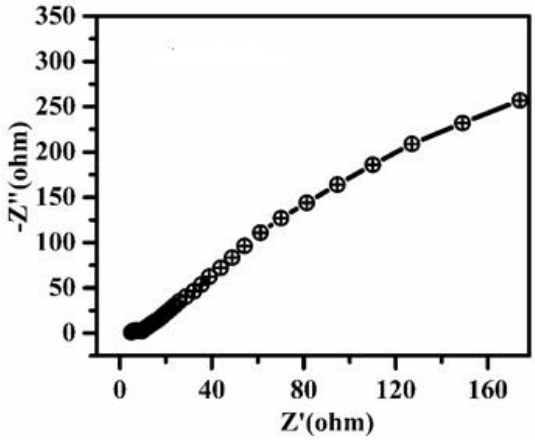

Figure 3

Figure 1: XRD plot of NiO
Figure 2: (a) CV curve of Nickel Oxide nanoparticles at different scan rates 10, 20, 30, 40, 50 and 60 mVs^{-1} in 1 M KOH electrolyte
Figure 2: (b) Galvanostatic charging and discharging at different current densities 1.00, 1.25, 1.50, 1.75, 2.00 and 2.25 Ag^{-1}
Figure 2: (c) Specific Capacitance as a function of varying current densities.
Figure 2: (d) Energy density versus power density plot.
Figure 3: Ragone plot of Nickel Oxide nanoparticles.